

Realization of the Werner-Holevo and Landau-Streater quantum channels for qutrits on quantum computers

A. I. Pakhomchik,¹ I. Feshchenko,^{2,1} A. Glatz,³ V. M. Vinokur,³ A. V. Lebedev,¹ K. V. Kuzhamuratova,¹ S. N. Filippov,^{1,4,5} and G. B. Lesovik¹

¹*Moscow Institute of Physics and Technology, Institutskii Per. 9, Dolgoprudny, Moscow Region 141700, Russia*

²*Skolkovo Institute of Science and Technology, 5 Nobelya str., Mozhauskij region, Moscow, 121205, Russia*

³*Materials Science Division, Argonne National Laboratory, 9700 S. Cass Avenue, Argonne, IL 60439, USA*

⁴*Steklov Mathematical Institute of Russian Academy of Sciences, Gubkina St. 8, Moscow 119991, Russia*

⁵*Valiev Institute of Physics and Technology of Russian Academy of Sciences, Nakhimovskii Pr. 34, Moscow 117218, Russia*

We realize Landau-Streater (LS) and Werner-Holevo (WH) quantum channels for qutrits on the IBM quantum computers. These channels correspond to interaction between the qutrit and its environment that result in the globally unitarily covariant qutrit transformation violating multiplicativity of the maximal p -norm. Our realization of LS and WH channels is based on embedding qutrit states into states of two qubits and using single-qubit and two-qubit CNOT gates to implement the specific interaction. We employ the standard quantum gates hence the developed algorithm suits any quantum computer. We run our algorithm on a 5-qubit and a 20-qubit computer as well as on a simulator. We quantify the quality of the implemented channels comparing their action on different input states with theoretical predictions. The overall efficiency is quantified by fidelity between the theoretical and experimental Choi states implemented on the 20-qubit computer.

I. INTRODUCTION

A quantum channel (QC) is a completely positive trace-preserving (CPTP) map, Φ , between operators $\mathcal{B}(\mathcal{H}_d)$ defined on the Hilbert space \mathcal{H}_d . Quantum channels conveniently describe the transformation of a density matrix, ρ , interacting with an environment¹⁻⁴. Unitary evolution of the closed system $\rho \rightarrow U\rho U^\dagger$ is an example of the QC that preserves the maximally mixed state $(1/d)\mathbf{I}$, i.e., $\Phi(\frac{1}{d}\mathbf{I}) = \frac{1}{d}\mathbf{I}$. It is shown⁵ that any open quantum dynamics of a qubit that preserves the maximally mixed state is an essentially random unitary one, $\rho \rightarrow \sum_i p_i U_i \rho U_i^\dagger$, however, in larger dimensions this is not the case. Namely, for a qutrit ($d=3$) there exists a quantum channel Φ such that $\Phi(\frac{1}{d}\mathbf{I}) = \frac{1}{d}\mathbf{I}$ but Φ is not random unitary⁵⁻⁷, and those are just the LS⁵ and WH⁸ channels that satisfy this condition. Furthermore, these qutrit channels are extremal, exhibit the global unitary covariance, and violate the multiplicativity of the maximal p -norm (see⁸ and⁹ for a review). Landau-Streater and Werner-Holevo channels hold high potential for applications in quantum information sciences. In this paper, we follow the experimental study of QC on quantum computers¹⁰⁻¹⁶ and implement the Landau-Streater and Werner-Holevo quantum channels for qutrits on IBM quantum computers with 5 and 20 qubits.

We realize the LS and WH channels using only one-qubit and CNOT gates. As shown in¹, any unitary operation can be approximated using these gates up to arbitrary accuracy. We represent a qutrit, a quantum state being equivalent to a particle with spin $s = 1$, as two qubits ignoring the highest energy level $|0\rangle_3 \rightarrow |00\rangle, |1\rangle_3 \rightarrow |01\rangle, |2\rangle_3 \rightarrow |10\rangle$. Since the used quantum computers, IBM QUANTUM EXPERIENCE¹⁷, are not perfect and are subject to a noise, the final density ma-

trix may have a non-zero probability of being in the ignored state. For example, a density matrix can transform into the following one: $\rho = (1 - \epsilon)\rho_{\text{qutrit}} + \epsilon(|11\rangle\langle 11| + |11\rangle\langle 10| + h.c.)$. We discard the last term and normalize ρ with respect to its trace, i.e., we consider only a qutrit part of the density matrix ($\rho \rightarrow \rho_{\text{qutrit}}$). We construct the Choi matrix corresponding to the QCs from the output density matrices using different input states. According to the Choi-Jamiołkowski isomorphism^{18,19}, the Choi matrix contains all information about the considered channel. We compare the obtained matrices with the theoretical expectations obtained by using a simulator of an ideal quantum computer, which is free of measurement errors and other types of errors related to the coupling to the environment. Finally, as a main result, we find that all the tomography experiments for the Werner-Holevo $\Phi_{WH}[\rho]$ and Landau-Streater $\Phi_{LS}[\rho]$ channels agree with the theoretical expectations.

II. BRIEF DESCRIPTION OF THE LANDAU-STREATER CHANNEL

The Landau-Streater channel Φ acts on the state ρ as follows

$$\Phi[\rho] = \frac{1}{s(s+1)}(J_x \rho J_x + J_y \rho J_y + J_z \rho J_z), \quad (1)$$

and is defined through the $SU(2)$ generators J_x, J_y, J_z acting on a $(2s+1)$ -dimensional Hilbert space \mathcal{H}_{2s+1} for a spin- s particle. In the case of a qutrit, $s = 1$, we define

the generators as²⁰:

$$J_x = \begin{pmatrix} 0 & \frac{1}{\sqrt{2}} & 0 \\ \frac{1}{\sqrt{2}} & 0 & \frac{1}{\sqrt{2}} \\ 0 & \frac{1}{\sqrt{2}} & 0 \end{pmatrix}; J_y = \begin{pmatrix} 0 & -\frac{i}{\sqrt{2}} & 0 \\ \frac{i}{\sqrt{2}} & 0 & -\frac{i}{\sqrt{2}} \\ 0 & \frac{i}{\sqrt{2}} & 0 \end{pmatrix};$$

$$J_z = \begin{pmatrix} 1 & 0 & 0 \\ 0 & 0 & 0 \\ 0 & 0 & -1 \end{pmatrix}. \quad (2)$$

In⁹, the Stinespring representation for the LS channel was derived and relevant matrices $\rho_{\text{env}} \in \mathcal{B}(\mathcal{H}_{\text{env}})$ and $U, \mathcal{H} \otimes \mathcal{H}_{\text{env}} \rightarrow \mathcal{H} \otimes \mathcal{H}_{\text{env}}$, were calculated and shown to satisfy the following equation:

$$\Phi[\rho] = \text{Tr}_{\text{env}}(U(\rho \otimes \rho_{\text{env}})U^\dagger), \quad (3)$$

yielding

$$\rho_{\text{env}} = |0\rangle\langle 0| \quad (4)$$

and

$$U = \left(\begin{array}{ccc|ccc|ccc} 0 & 0 & 0 & \frac{1}{2} & 0 & 0 & 0 & \frac{i}{\sqrt{2}} & -\frac{i}{2} \\ 0 & 0 & \frac{i}{\sqrt{2}} & -\frac{i}{2} & 0 & 0 & 0 & 0 & \frac{1}{2} \\ \frac{1}{\sqrt{2}} & 0 & 0 & 0 & \frac{i}{2} - \frac{1}{2\sqrt{2}} & -\frac{i}{2\sqrt{2}} & 0 & 0 & 0 \\ \hline \frac{1}{2} & 0 & 0 & 0 & \frac{1}{2} - \frac{i}{2\sqrt{2}} & \frac{1}{2\sqrt{2}} & \frac{1}{2} & 0 & 0 \\ \frac{i}{2} & 0 & 0 & 0 & \frac{1}{2\sqrt{2}} & -\frac{1}{2} - \frac{i}{2\sqrt{2}} & -\frac{i}{2} & 0 & 0 \\ 0 & 1 & 0 & 0 & 0 & 0 & 0 & 0 & 0 \\ \hline 0 & 0 & \frac{1}{\sqrt{2}} & \frac{1}{2} & 0 & 0 & 0 & 0 & \frac{i}{2} \\ 0 & 0 & 0 & \frac{i}{2} & 0 & 0 & 0 & \frac{1}{\sqrt{2}} & \frac{1}{2} \\ 0 & 0 & 0 & 0 & \frac{1}{2\sqrt{2}} & \frac{1}{2} - \frac{i}{2\sqrt{2}} & -\frac{1}{\sqrt{2}} & 0 & 0 \end{array} \right). \quad (5)$$

III. EMULATION OF QUTRITS BY QUBITS

The Kraus rank of the LS channel is 3, so one needs at least the three-dimensional environment. The Hilbert space of two qutrits $\mathcal{H} \otimes \mathcal{H}_{\text{env}} = \mathcal{H}_{2s+1} \otimes \mathcal{H}_{2s+1}$ (where $s = 1$) has 3^2 basis states and the Hilbert space of N qubits has 2^N basis states. Therefore, one needs $N = 4$ qubits for the 9 states of two qutrits, which are sufficient to encode a system qutrit that is transformed by the channel and a separate environment qutrit. In other words, one qutrit uses one pair of qubits, and the other qutrit uses another pair.

For encoding three logical states $m_s = -1$, $m_s = 0$, and $m_s = 1$ of a qutrit we use the states $|00\rangle$, $|01\rangle$, and $|10\rangle$, respectively. This choice is related to the fact that the quantum computer is not perfect, meaning that excited states may over time evolve back into the ground states due to the amplitude-damping noise. We did not use physical two-qubit state $|11\rangle$, because it has the highest energy and, therefore, the shortest relaxation time into other states. It can decay into the two states, $|01\rangle$ and $|10\rangle$, which in their turn can only return to ground

state $|00\rangle$. In summary, the algorithm that transforms $\{|00\rangle, |01\rangle, |10\rangle\} \otimes \{|00\rangle, |01\rangle, |10\rangle\}$ states by U and acts trivially on the other non-qutrit state has the following matrix:

$$\left(\begin{array}{ccc|ccc|ccc|ccc} 0 & 0 & 0 & \frac{1}{2} & 0 & 0 & 0 & \frac{i}{\sqrt{2}} & -\frac{i}{2} & 0 & 0 & 0 \\ 0 & 0 & \frac{i}{\sqrt{2}} & -\frac{i}{2} & 0 & 0 & 0 & 0 & 0 & \frac{1}{2} & 0 & 0 \\ \frac{1}{\sqrt{2}} & 0 & 0 & 0 & \frac{i}{2} - \frac{1}{2\sqrt{2}} & -\frac{i}{2\sqrt{2}} & 0 & 0 & 0 & 0 & 0 & 0 \\ \hline 0 & 0 & 0 & 1 & 0 & 0 & 0 & 0 & 0 & 0 & 0 & 0 \\ \hline \frac{1}{2} & 0 & 0 & 0 & \frac{1}{2} - \frac{i}{2\sqrt{2}} & \frac{1}{2\sqrt{2}} & 0 & \frac{1}{2} & 0 & 0 & 0 & 0 \\ \frac{i}{2} & 0 & 0 & 0 & 0 & \frac{1}{2\sqrt{2}} & -\frac{1}{2} - \frac{i}{2\sqrt{2}} & -\frac{i}{2} & 0 & 0 & 0 & 0 \\ 0 & 1 & 0 & 0 & 0 & 0 & 0 & 0 & 0 & 0 & 0 & 0 \\ \hline 0 & 0 & 0 & 0 & 0 & 0 & 1 & 0 & 0 & 0 & 0 & 0 \\ \hline 0 & 0 & \frac{1}{\sqrt{2}} & 0 & \frac{1}{2} & 0 & 0 & 0 & 0 & \frac{i}{2} & \frac{1}{2} & 0 \\ 0 & 0 & 0 & 0 & \frac{i}{2} & 0 & 0 & 0 & \frac{1}{\sqrt{2}} & \frac{1}{2} & 0 & 0 \\ 0 & 0 & 0 & 0 & 0 & \frac{1}{2\sqrt{2}} & \frac{1}{2} - \frac{i}{2\sqrt{2}} & -\frac{1}{\sqrt{2}} & 0 & 0 & 0 & 0 \\ \hline 0 & 0 & 0 & 0 & 0 & 0 & 0 & 0 & 0 & 1 & 0 & 0 \\ \hline \hat{0} & \hat{0} & \hat{0} & \hat{0} & \hat{0} & \hat{0} & \hat{0} & \hat{0} & \hat{0} & \hat{0} & \hat{1} & \hat{1} \end{array} \right), \quad (6)$$

where $\hat{0} = \begin{pmatrix} 0 & 0 & 0 & 0 \\ 0 & 0 & 0 & 0 \\ 0 & 0 & 0 & 0 \\ 0 & 0 & 0 & 0 \end{pmatrix}$, $\hat{1} = \begin{pmatrix} 1 & 0 & 0 & 0 \\ 0 & 1 & 0 & 0 \\ 0 & 0 & 1 & 0 \\ 0 & 0 & 0 & 1 \end{pmatrix}$, $\mathbf{0} = \begin{pmatrix} 0 & 0 & 0 \\ 0 & 0 & 0 \end{pmatrix}$.

IV. IMPLEMENTATION OF THE LANDAU-STREATER CHANNEL THROUGH THE WERNER-HOLEVO CHANNEL

By definition, the WH channel⁸ transforms the density matrix ($\rho \in \mathcal{B}(\mathcal{H}_d)$) as follows:

$$\Phi_{\text{WH}}[\rho] = \frac{1}{d-1}(\text{Tr}[\rho]I - \rho^T). \quad (7)$$

After the unitary transformation

$$W = \begin{pmatrix} 0 & 0 & 1 \\ 0 & -1 & 0 \\ 1 & 0 & 0 \end{pmatrix}, \quad (8)$$

we get, accordingly, the LS channel:

$$\Phi_{\text{LS}}[\rho] = \Phi_{\text{WH}}[W\rho W^\dagger]. \quad (9)$$

The WH channel can be represented as

$$\Phi_{\text{WH}}[\rho] = \text{Tr}_{\text{env}}(U(\rho_{\text{env}} \otimes \rho)U^\dagger), \quad (10)$$

where

$$\rho_{\text{env}} = |0\rangle\langle 0|, \quad (11)$$

and

$$U = \frac{1}{\sqrt{2}} \left(\begin{array}{ccc|cc} 0 & 1 & 0 & & \\ -1 & 0 & 0 & U_{-1;0} & U_{-1;1} \\ 0 & 0 & 0 & & \\ \hline 0 & 0 & 1 & & \\ 0 & 0 & 0 & U_{0;0} & U_{0;1} \\ -1 & 0 & 0 & & \\ \hline 0 & 0 & 0 & & \\ 0 & 0 & 1 & U_{1;0} & U_{1;1} \\ 0 & -1 & 0 & & \end{array} \right). \quad (12)$$

The only requirement for the $\{U_{m_j;0}\}$ and $\{U_{m_j;1}\}$ blocks is that U is unitary.

This can be decomposed into elementary gates:

$$\begin{aligned} W &= \begin{pmatrix} 0 & 0 & 1 & 0 \\ 0 & -1 & 0 & 0 \\ 1 & 0 & 0 & 0 \\ 0 & 0 & 0 & -1 \end{pmatrix} = \begin{pmatrix} 1 & 0 & 0 & 0 \\ 0 & -1 & 0 & 0 \\ 0 & 0 & 1 & 0 \\ 0 & 0 & 0 & -1 \end{pmatrix} \begin{pmatrix} 0 & 0 & 1 & 0 \\ 0 & 0 & 0 & 1 \\ 1 & 0 & 0 & 0 \\ 0 & 1 & 0 & 0 \end{pmatrix} \begin{pmatrix} 1 & 0 & 0 & 0 \\ 0 & 0 & 0 & 1 \\ 0 & 0 & 1 & 0 \\ 0 & 1 & 0 & 0 \end{pmatrix} \begin{pmatrix} 0 & 0 & 1 & 0 \\ 0 & 0 & 0 & 1 \\ 1 & 0 & 0 & 0 \\ 0 & 1 & 0 & 0 \end{pmatrix} = \\ &= Z_2 \times X_2 \times \text{CNOT}_{21} \times X_2 = i(Y_2 \times \text{CNOT}_{21} \times X_2), \end{aligned} \quad (14)$$

where X_k, Y_k, Z_k are Pauli gates acting on k -th qubit, and CNOT_{kl} means CNOT gate where k -th qubit is a control qubit and l -th is the target qubit.

For the effective decomposition into one-qubit gates, we replace the Toffoli gate by a quasi-Toffoli one. It requires fewer CNOT gates (Fig. 1) and has the following matrix:

$$\begin{pmatrix} 1 & 0 & 0 & 0 & 0 & 0 & 0 & 0 \\ 0 & 1 & 0 & 0 & 0 & 0 & 0 & 0 \\ 0 & 0 & 1 & 0 & 0 & 0 & 0 & 0 \\ 0 & 0 & 0 & 1 & 0 & 0 & 0 & 0 \\ 0 & 0 & 0 & 0 & -1 & 0 & 0 & 0 \\ 0 & 0 & 0 & 0 & 0 & 1 & 0 & 0 \\ 0 & 0 & 0 & 0 & 0 & 0 & 0 & 1 \\ 0 & 0 & 0 & 0 & 0 & 0 & 1 & 0 \end{pmatrix}. \quad (15)$$

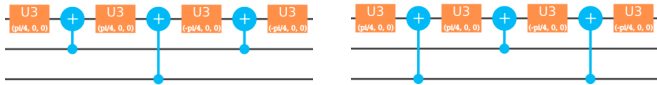


FIG. 1. Two different implementations of a quasi-Toffoli gate.

In the matrix emulation, see Sec. IV, by qubits that is described in Sec. III, the impact on the unused state (which does not encode a logical qutrit) could be any if it preserves the unitarity of the matrix. Taking advantage

With the selected method of encoding logical states of a qutrit by two qubits we implement the transformation W as follows:

$$\widetilde{W} = \begin{pmatrix} 0 & 0 & 1 & 0 \\ 0 & -1 & 0 & 0 \\ 1 & 0 & 0 & 0 \\ 0 & 0 & 0 & e^{i\varphi} \end{pmatrix}. \quad (13)$$

of this condition, we represent the matrix for Werner-Holevo channel as:

$$\widetilde{U} = \frac{1}{\sqrt{2}} \left(\begin{array}{ccc|cc} 0 & 1 & 0 & & \\ -1 & 0 & 0 & & \\ 0 & 0 & 0 & & \\ 0 & 0 & 0 & & \\ \hline 0 & 0 & 1 & & \\ 0 & 0 & 0 & & \\ -1 & 0 & 0 & & \\ 0 & 0 & 0 & & \\ \hline 0 & 0 & 0 & \widetilde{U}' & \\ 0 & 0 & 0 & & \\ 0 & 0 & 1 & & \\ 0 & -1 & 0 & & \\ 0 & 0 & 0 & & \\ \hline 0 & 0 & 0 & & \\ 0 & 0 & 0 & & \\ 0 & 0 & 0 & & \\ 0 & 0 & 0 & & \end{array} \right). \quad (16)$$

The columns of \widetilde{U}' are arbitrary except that the \widetilde{U} matrix must satisfy the unitary constraint. Using the quasi-Toffoli and CNOT gates, we make lines permutations, S , (Fig. 2) of the \widetilde{U} matrix such that its absolute values are equal to a tensor product of one-qubit gates.

As a result, we get the following matrix:

$$S\tilde{U} = \frac{1}{\sqrt{2}} \left(\begin{array}{ccc|ccc} 0 & 0 & 0 & 0 & 0 & 0 \\ 0 & 0 & 1 & 0 & 0 & 0 \\ 0 & 1 & 0 & 0 & 0 & 0 \\ -1 & 0 & 0 & 0 & 0 & 0 \\ \hline 0 & 0 & 0 & 0 & 0 & 0 \\ 0 & 0 & 0 & 0 & 0 & 0 \\ 0 & 0 & 0 & 0 & 0 & 0 \\ 0 & 0 & 0 & 0 & 0 & 0 \\ 0 & 0 & 0 & 0 & 0 & 0 \\ 0 & 0 & 0 & 0 & 0 & 0 \\ 0 & -1 & 0 & 0 & 0 & 0 \\ -1 & 0 & 0 & 0 & 0 & 0 \\ \hline 0 & 0 & 0 & 0 & 0 & 0 \\ 0 & 0 & 0 & 0 & 0 & 0 \\ 0 & 0 & 1 & 0 & 0 & 0 \\ 0 & -1 & 0 & 0 & 0 & 0 \\ -1 & 0 & 0 & 0 & 0 & 0 \end{array} \right) S\tilde{U}', \quad (17)$$

which is almost equal (some elements might have different phases because we used the quasi-Toffoli gate instead the Toffoli one) to:

$$\frac{1}{\sqrt{2}} \left(\begin{array}{cc|cc|cc|cc} \mathbf{0} & \hat{\sigma}_x & \mathbf{0} & \mathbf{0} & \mathbf{0} & \hat{\sigma}_x & \mathbf{0} & \mathbf{0} & \mathbf{0} & \mathbf{0} \\ \hat{\sigma}_x & \mathbf{0} & \mathbf{0} & \mathbf{0} & \hat{\sigma}_x & \mathbf{0} & \mathbf{0} & \mathbf{0} & \mathbf{0} & \mathbf{0} \\ \hline \mathbf{0} & \mathbf{0} & \mathbf{0} & \hat{\sigma}_x & \mathbf{0} & \mathbf{0} & \mathbf{0} & \mathbf{0} & \mathbf{0} & \hat{\sigma}_x \\ \mathbf{0} & \mathbf{0} & \hat{\sigma}_x & \mathbf{0} & \mathbf{0} & \mathbf{0} & \hat{\sigma}_x & \mathbf{0} & \mathbf{0} & \mathbf{0} \\ \hline \mathbf{0} & \hat{\sigma}_x & \mathbf{0} & \mathbf{0} & \mathbf{0} & -\hat{\sigma}_x & \mathbf{0} & \mathbf{0} & \mathbf{0} & \mathbf{0} \\ \hat{\sigma}_x & \mathbf{0} & \mathbf{0} & \mathbf{0} & -\hat{\sigma}_x & \mathbf{0} & \mathbf{0} & \mathbf{0} & \mathbf{0} & \mathbf{0} \\ \hline \mathbf{0} & \mathbf{0} & \mathbf{0} & \hat{\sigma}_x & \mathbf{0} & \mathbf{0} & \mathbf{0} & \mathbf{0} & \mathbf{0} & -\hat{\sigma}_x \\ \mathbf{0} & \mathbf{0} & \hat{\sigma}_x & \mathbf{0} & \mathbf{0} & \mathbf{0} & \mathbf{0} & \mathbf{0} & -\hat{\sigma}_x & \mathbf{0} \end{array} \right) =$$

$$= \mathbf{H} \otimes \mathbf{Id} \otimes \hat{\sigma}_x \otimes \hat{\sigma}_x =$$

$$= \left(\frac{1}{\sqrt{2}} \begin{pmatrix} 1 & 1 \\ 1 & -1 \end{pmatrix} \right) \otimes \begin{pmatrix} 1 & 0 \\ 0 & 1 \end{pmatrix} \otimes \begin{pmatrix} 0 & 1 \\ 1 & 0 \end{pmatrix} \otimes \begin{pmatrix} 0 & 1 \\ 1 & 0 \end{pmatrix}. \quad (18)$$

A decomposition into a tensor product of simple gates exist only in 4 out of 8 cases (Fig. 3):

$$S_1\tilde{U} = \left(\frac{1}{\sqrt{2}} \begin{pmatrix} 1 & 1 \\ -1 & 1 \end{pmatrix} \right) \otimes \begin{pmatrix} 1 & 0 \\ 0 & 1 \end{pmatrix} \otimes \begin{pmatrix} 0 & 1 \\ 1 & 0 \end{pmatrix} \otimes \begin{pmatrix} 0 & 1 \\ -1 & 0 \end{pmatrix}, \quad (19)$$

$$S_2\tilde{U} = \left(\frac{1}{\sqrt{2}} \begin{pmatrix} 1 & 1 \\ -1 & 1 \end{pmatrix} \right) \otimes \begin{pmatrix} 1 & 0 \\ 0 & 1 \end{pmatrix} \otimes \begin{pmatrix} 0 & 1 \\ 1 & 0 \end{pmatrix} \otimes \begin{pmatrix} 0 & 1 \\ -1 & 0 \end{pmatrix}, \quad (20)$$

$$S_3\tilde{U} = \left(\frac{1}{\sqrt{2}} \begin{pmatrix} 1 & 1 \\ 1 & -1 \end{pmatrix} \right) \otimes \begin{pmatrix} 1 & 0 \\ 0 & 1 \end{pmatrix} \otimes \begin{pmatrix} 0 & 1 \\ 1 & 0 \end{pmatrix} \otimes \begin{pmatrix} 0 & -1 \\ 1 & 0 \end{pmatrix}, \quad (21)$$

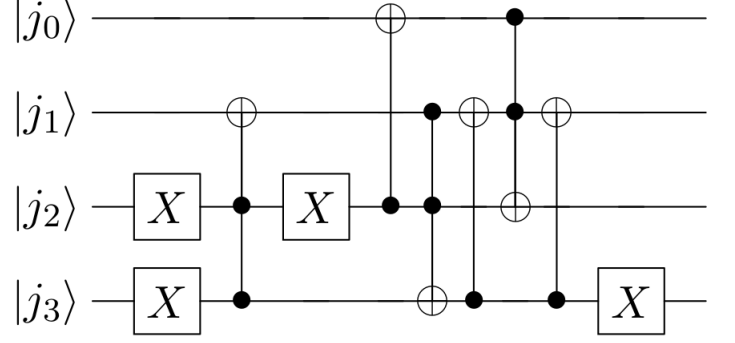


FIG. 2. Algorithm for line permutations. Qubits $|j_2\rangle$ and $|j_3\rangle$ encode the environment qutrit and qubits $|j_0\rangle$ and $|j_1\rangle$ encode the channel-transformed spin-1 particle.

$$S_4\tilde{U} = \left(\frac{1}{\sqrt{2}} \begin{pmatrix} 1 & 1 \\ 1 & -1 \end{pmatrix} \right) \otimes \begin{pmatrix} 1 & 0 \\ 0 & 1 \end{pmatrix} \otimes \begin{pmatrix} 0 & 1 \\ 1 & 0 \end{pmatrix} \otimes \begin{pmatrix} 0 & -1 \\ 1 & 0 \end{pmatrix}. \quad (22)$$

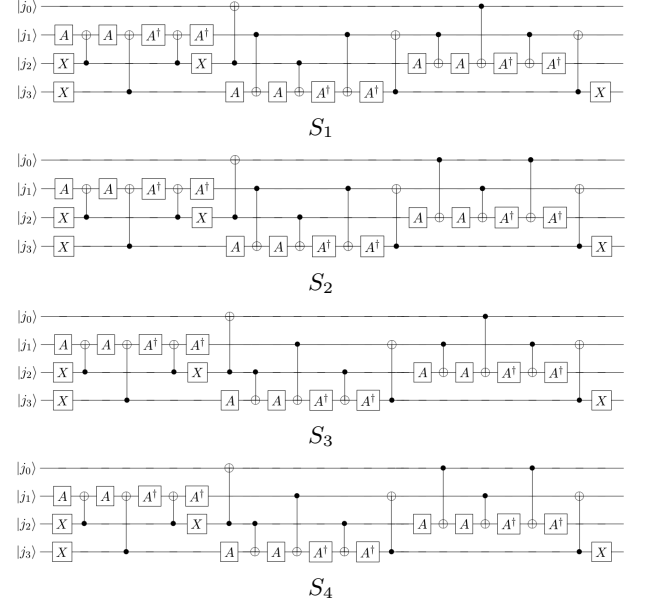


FIG. 3. Implementations of the algorithm shown in Fig. 2, using the CNOT decomposition of quasi-Toffoli gates. Here

$$A = U_3(\pi/4, 0, 0) = \begin{pmatrix} \cos(\frac{\pi}{8}) & -\sin(\frac{\pi}{8}) \\ \sin(\frac{\pi}{8}) & \cos(\frac{\pi}{8}) \end{pmatrix}.$$

Not every CNOT gate can be performed on IBM quantum computers due to missing connections, see connectivity map for the 5-qubit machine in Fig. 4 and 20-qubit machine in Fig. 6.

On the 5-qubit machine each couple of qubits in the coupling map has only one target and control qubit. Therefore, if we need to swap the control and target

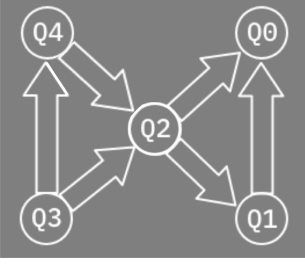


FIG. 4. Coupling map of two-qubit gates on a 5-qubit machine

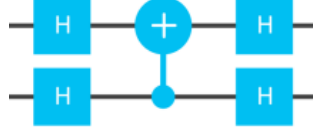


FIG. 5. Swap algorithm for the target and control qubits of a CNOT gate.

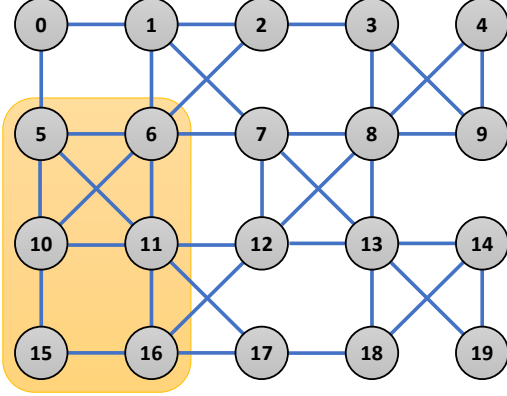


FIG. 6. Connectivity map of IBM's 20-qubit machine tokyo. The (yellow) highlighted qubits were used to implement the quantum channels.

qubit, we need to use the method shown in Fig. 5 adding Hadamard gates. We choose a configuration in the Fig. 2 such that the number of two-qubit CNOT gates is minimal because CNOT gate has the greatest error.

On this machine, we use the S_4 configuration implementing the Werner-Holevo channel. The sequence of gates for this is shown in figure 7 ($U1(\lambda)$, $U2(\varphi, \lambda)$, and $U3(\theta, \varphi, \lambda)$ are a full set of one-qubit gates on IBM machines). Qubits $|q3, q0\rangle$ encode $|j0, j1\rangle$ (channel qubits) and $|q2, q1\rangle$ represent $|j2, j3\rangle$ (environment qubits).

The \tilde{W} transformation requires a CNOT gate between the system qubits ($|q3, q0\rangle$). However, the coupling map of the 5-qubit machine does not allow to place a CNOT operator there. Therefore, we have to use three CNOT gates instead of a single one and place them in accordance with the coupling map (Fig. 4).

Finally, we realize the unitary interaction U (formula 5) with the use of $S_4\tilde{U}$ (Fig. 7) and \tilde{W} transformations (Fig. 8).

V. MEASUREMENTS

In order to predict the final quantum state for an arbitrary initial state, we performed the transformation of

each basis density matrix per channel. Explicitly, we use the following 9 matrices as inputs:

$$\begin{aligned} \rho_1 &= \begin{pmatrix} 1 & 0 & 0 \\ 0 & 0 & 0 \\ 0 & 0 & 0 \end{pmatrix}, & \rho_2 &= \begin{pmatrix} 0 & 0 & 0 \\ 0 & 1 & 0 \\ 0 & 0 & 0 \end{pmatrix}, & \rho_3 &= \begin{pmatrix} 0 & 0 & 0 \\ 0 & 0 & 0 \\ 0 & 0 & 1 \end{pmatrix}, \\ \rho_4 &= \frac{1}{2} \begin{pmatrix} 1 & 1 & 0 \\ 1 & 1 & 0 \\ 0 & 0 & 0 \end{pmatrix}, & \rho_5 &= \frac{1}{2} \begin{pmatrix} 1 & 0 & 1 \\ 0 & 0 & 0 \\ 1 & 0 & 1 \end{pmatrix}, & \rho_6 &= \frac{1}{2} \begin{pmatrix} 0 & 0 & 0 \\ 0 & 1 & 1 \\ 0 & 1 & 1 \end{pmatrix}, \\ \rho_7 &= \frac{1}{2} \begin{pmatrix} 1 & -i & 0 \\ i & 1 & 0 \\ 0 & 0 & 0 \end{pmatrix}, & \rho_8 &= \frac{1}{2} \begin{pmatrix} 1 & 0 & -i \\ 0 & 0 & 0 \\ i & 0 & 1 \end{pmatrix}, & \rho_9 &= \frac{1}{2} \begin{pmatrix} 0 & 0 & 0 \\ 0 & 1 & -i \\ 0 & i & 1 \end{pmatrix} \end{aligned} \quad (23)$$

After the transformation by the channel, we perform a tomography²¹ of the system qutrit. Knowing these density matrices, we can reconstruct a channel using its linear property:

$$\Phi \left(\sum_i a_i \rho_i \right) = \sum_i a_i \Phi(\rho_i). \quad (24)$$

Any of basis states can be prepared using unitary transformations, see Fig. 9 (where $\rho_k = |\psi_k\rangle \langle \psi_k|$).

In practice, IBM has implemented the tomography algorithm in their python library (QISKit²²). We use it instead of our own realization.

As a quality test, we use the following expression to calculate the fidelity²³ between the theoretical and experimental output density matrix for same inputs:

$$F(\sigma_1, \sigma_2) = \left(\text{Tr} \sqrt{\sqrt{\sigma_1} \sigma_2 \sqrt{\sigma_1}} \right)^2, \quad (25)$$

where $F(\sigma_1, \sigma_2) = F(\sigma_2, \sigma_1)$.

The QISKit²² toolkit also includes a simulator of an ideal quantum computer, which has no measurement or environment coupling errors. We thus obtain the theoretically expected results. Results of all tomography experiments on simulator for the WH $\Phi_{\text{WH}}[\rho_i]$ and LS $\Phi_{\text{LS}}[\rho_i]$ channels fit well to the theoretical expectations (fidelity of both channels is nearly 0.99).

VI. CHOI MATRIX OF THE LANDAU-STREATER CHANNEL AND COMPARISON WITH THEORETICAL EXPECTATIONS

Any quantum channel acting on the Hilbert space \mathcal{H}_N is connected to a linear map in $\mathcal{H}_N \otimes \mathcal{H}_N$ (Choi-Jamiołkowski isomorphism). The duality between channels and states refers to the map:

$$\Phi \rightarrow \Omega = (Id \otimes \Phi)(|\psi_+\rangle \langle \psi_+|), \quad (26)$$

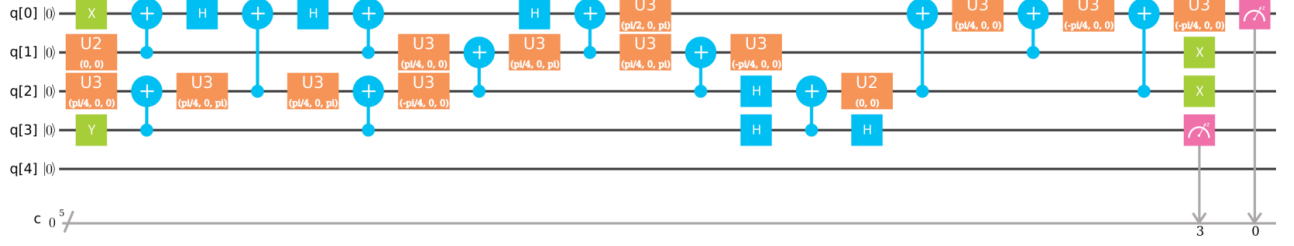


FIG. 7. Implementation of the S_4 configuration (Fig. 2) on a 5-qubit machine regarding its coupling map.

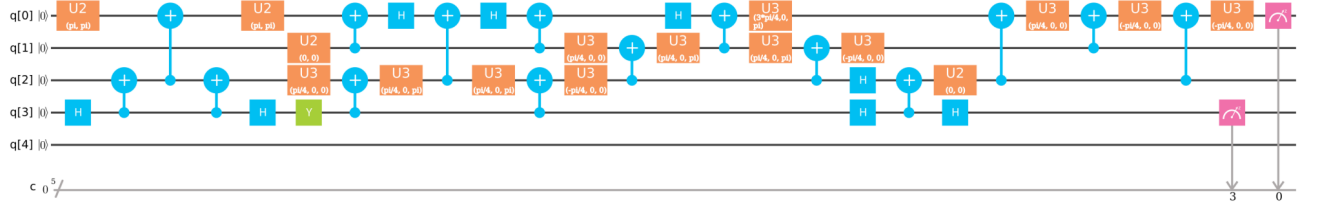


FIG. 8. Realization of Landau-Streater channel based on the Werner-Holevo channel.

where Φ is the quantum channel, Id the identity channel ($\forall \rho \in \mathcal{B}(\mathcal{H}_N) : Id(\rho) = \rho$), and $|\psi_+\rangle = \frac{1}{\sqrt{N}} \sum_{i=1}^N |i\rangle |i\rangle$.

ing expression:

$$\begin{aligned}
 \Omega &= (Id \otimes \Phi)(|\psi_+\rangle \langle \psi_+|) = \\
 &= \frac{1}{N} (Id \otimes \Phi) \left(\sum_{i=1}^N \sum_{k=1}^N |i\rangle |i\rangle \langle k| \langle k| \right) = \\
 &= \frac{1}{N} (Id \otimes \Phi) \left(\sum_{i=1}^N \sum_{k=1}^N |i\rangle \langle k| \otimes |i\rangle \langle k| \right) = \\
 &= \frac{1}{N} \sum_{i=1}^N \sum_{k=1}^N |i\rangle \langle k| \otimes \Phi(|i\rangle \langle k|). \quad (27)
 \end{aligned}$$

This formula allows one to restore the Choi matrix by measuring final states. As one sees, $|i\rangle \langle k|$ products might not be the density operators ($\text{Tr } |i\rangle \langle k| = 0$, if $i \neq k$). But each term $|i\rangle \langle k|$ can be represented as a linear combination of physical matrices. For convenience, $E_{i,j}$ denotes $|i\rangle \langle j|$. In case the dimension is equal to 3, we get follow-

$$\begin{aligned}
 E_{i,j} &= \begin{pmatrix} |0\rangle \langle 0| \\ |0\rangle \langle 1| \\ |0\rangle \langle 2| \\ |1\rangle \langle 0| \\ |1\rangle \langle 1| \\ |1\rangle \langle 2| \\ |2\rangle \langle 0| \\ |2\rangle \langle 1| \\ |2\rangle \langle 2| \end{pmatrix} = \sum_{k=1}^9 a_{i,j}^k \cdot \mathfrak{R}_k = \\
 &= \begin{pmatrix} 1 & 0 & 0 & 0 & 0 & 0 & 0 & 0 & 0 \\ -\frac{1+i}{2} & -\frac{1+i}{2} & 0 & 1 & 0 & 0 & i & 0 & 0 \\ -\frac{1+i}{2} & 0 & -\frac{1+i}{2} & 0 & 1 & 0 & 0 & i & 0 \\ -\frac{1-i}{2} & -\frac{1-i}{2} & 0 & 1 & 0 & 0 & -i & 0 & 0 \\ 0 & 1 & 0 & 0 & 0 & 0 & 0 & 0 & 0 \\ 0 & -\frac{1+i}{2} & -\frac{1+i}{2} & 0 & 0 & 1 & 0 & 0 & i \\ -\frac{1-i}{2} & 0 & -\frac{1-i}{2} & 0 & 1 & 0 & 0 & -i & 0 \\ 0 & -\frac{1-i}{2} & -\frac{1-i}{2} & 0 & 0 & 1 & 0 & 0 & -i \\ 0 & 0 & 1 & 0 & 0 & 0 & 0 & 0 & 0 \end{pmatrix} \cdot \mathfrak{R}_k, \quad (28)
 \end{aligned}$$

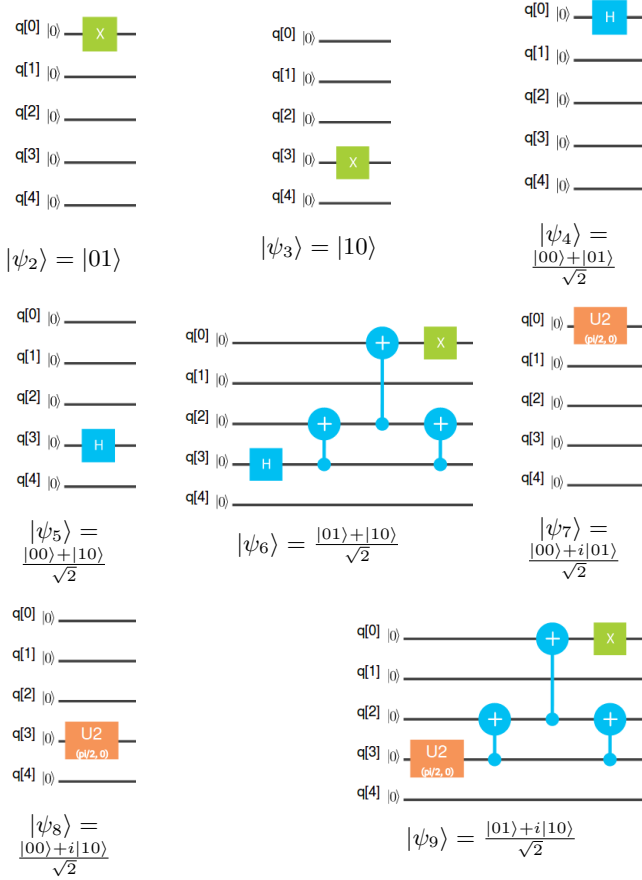


FIG. 9. Preparation of initial states. If all qubits were connected to each other on the 5-qubit machine, only one CNOT gate would be required for $|\psi_6\rangle$ and $|\psi_9\rangle$, but given the current coupling map, we need to use 3 CNOTs.

where $\mathfrak{R}_k = \begin{pmatrix} |0\rangle\langle 0| \\ |1\rangle\langle 1| \\ |2\rangle\langle 2| \\ \frac{1}{2}(|0\rangle + |1\rangle)(\langle 0| + \langle 1|) \\ \frac{1}{2}(|0\rangle + |2\rangle)(\langle 0| + \langle 2|) \\ \frac{1}{2}(|1\rangle + |2\rangle)(\langle 1| + \langle 2|) \\ \frac{1}{2}(|0\rangle + i|1\rangle)(\langle 0| - i\langle 1|) \\ \frac{1}{2}(|0\rangle + i|2\rangle)(\langle 0| - i\langle 2|) \\ \frac{1}{2}(|1\rangle + i|2\rangle)(\langle 1| - i\langle 2|) \end{pmatrix}$. Then, the Choi matrix Ω can be expressed as:

$$\Omega = \sum_{i=1}^N \sum_{j=1}^N E_{i,j} \otimes \Phi(E_{i,j}) = \sum_{i=1}^N \sum_{j=1}^N E_{i,j} \otimes \sum_{k=1}^{N^2} a_{i,j}^k \Phi(\mathfrak{R}_k). \quad (29)$$

For illustrative purposes, we present it as a block matrix:

$$\Omega = \begin{pmatrix} \sum_{k=1}^{N^2} a_{0,0}^k \Phi(\mathfrak{R}_k) & \sum_{k=1}^{N^2} a_{0,1}^k \Phi(\mathfrak{R}_k) & \sum_{k=1}^{N^2} a_{0,2}^k \Phi(\mathfrak{R}_k) \\ \sum_{k=1}^{N^2} a_{1,0}^k \Phi(\mathfrak{R}_k) & \sum_{k=1}^{N^2} a_{1,1}^k \Phi(\mathfrak{R}_k) & \sum_{k=1}^{N^2} a_{1,2}^k \Phi(\mathfrak{R}_k) \\ \sum_{k=1}^{N^2} a_{2,0}^k \Phi(\mathfrak{R}_k) & \sum_{k=1}^{N^2} a_{2,1}^k \Phi(\mathfrak{R}_k) & \sum_{k=1}^{N^2} a_{2,2}^k \Phi(\mathfrak{R}_k) \end{pmatrix} \quad (30)$$

Consequently, in order to build the Choi matrix Ω , it is sufficient to know how the channel acts on the basis matrices \mathfrak{R} .

The Choi state (26) cannot be physically realized on IBM a 5-qubit machine because needs an extra qutrit (plus 2 qubits and 6 qubits in total). The connectivity map of 15-qubit machines also does not allow a direct implementation. Only on a 20-qubit computer (see connectivity map in Fig 6) we can build the Choi matrix using formula (26). In order to be able to utilize the 5-qubit machine, we used another expression, Eqs. (29) & (30) to reconstruct the Choi matrix Ω .

5-qubit computer(ibmqx4)

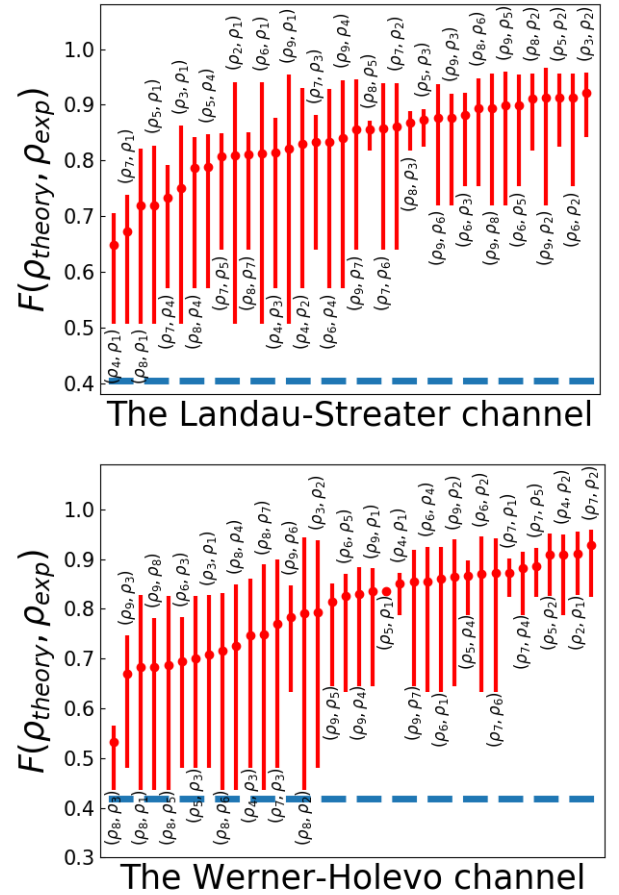


FIG. 10. Fidelity by pairs of density matrices. Every pair stick contains maximum, minimum, and average (a point on a stick) The dashed line represents the fidelity between theoretical and experimental Choi matrices Ω .

Using this procedure, we get the Choi matrices Ω for the Landau-Streater and Werner-Holevo channels. We compared them with the theoretical expectations, and obtained the values 0.406 and 0.419 for the fidelity ($F(\Omega_{\text{theory}}, \Omega_{\text{exp}}) = (\text{Tr} \sqrt{\sqrt{\Omega_{\text{theory}}} \Omega_{\text{exp}} \sqrt{\Omega_{\text{theory}}}})^2$), respectively.

Since the Choi matrix Ω contains all information about the channel map, we can reconstruct it according to the following expression:

$$\Phi(\rho) = \text{Tr}_1((\rho^\top \otimes \text{Id}) \cdot \Omega). \quad (31)$$

In figure 10, we show the fidelity between theoretical and experimental results for both channels. For each pair of the basis density matrices, we calculated the fidelity of $\lambda\rho_a + (1 - \lambda)\rho_b$ for $\forall \lambda \in [0, 1]$ using Eq. (31). Each bar for the pairs shows maximum, minimum, and average (point on the bar).

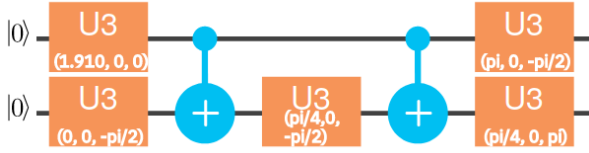


FIG. 11. Preparation of a qutrit superposition state $\frac{|00\rangle + |01\rangle + |10\rangle}{\sqrt{3}}$. 1.910 is the approximate value of $2 \arccos \frac{1}{\sqrt{3}}$.

In contrast to this more involved procedure, we built the Choi matrix straight forwardly using Eq. (26) on a 20-qubit computer (IBM machine tokyo). Its connectivity map is shown in Fig. 6, where we used the highlighted 6 qubits, which are sufficient for the required placement of CNOT gates. According to this expression, we need to prepare the state $|\psi_+\rangle = \frac{1}{\sqrt{3}} \sum_{i=1}^3 |i\rangle |i\rangle$, for which we first create the state $|\psi_{+s}\rangle = \frac{1}{\sqrt{3}} \sum_{i=1}^3 |i\rangle$ on our system qubits using the scheme of Fig. 11. Then, we place CNOT gates between system qubits and auxiliary qubits such that the control qubit is a system qubit and the target qubit is auxiliary. After these steps, we get the state $|\psi_+\rangle = \frac{1}{\sqrt{3}} \sum_{i=1}^3 |i\rangle |i\rangle$ and apply the Landau-Streater (Werner-Holevo) channel transformations on this state and perform the tomography. The results of these experiments are shown in Fig. 12.

VII. CONCLUSION

We developed and implemented algorithms for the Landau-Streater and Werner-Holevo channels. Experiments were carried out on the 5-qubit and 20-qubit quantum computers. The large errors encountered in the calculations can be mostly attributed to the CNOT gate errors, which have the largest error rate and are extensively used in the algorithm. In the future we expect

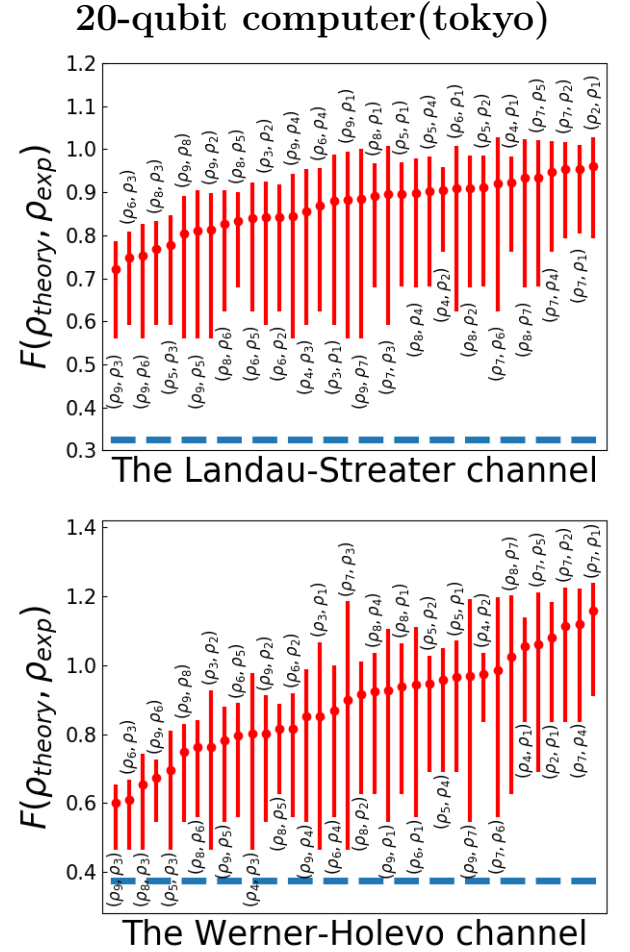


FIG. 12. Fidelity by pairs of density matrices. Each bar shows maximum, minimum, and average (point). The dashed line represents the fidelity between theoretical and experimental Choi matrices Ω .

to reduce the number of used CNOT gates and thus to increase the overall fidelity of the experiments.

ACKNOWLEDGMENTS

The research was supported by the Government of the Russian Federation (Agreement 05.Y09.21.0018), Russian Foundation for Basic Research grants Nos. 17-02-00396A, 18-02-00642A and 18-37-20073, Foundation for the Advancement of Theoretical Physics and Mathematics “BASIS”, the Ministry of Science and Higher Education of the Russian Federation (16.7162.2017/8.9 and Program No. 0066-2019-0005 for Valiev Institute of Physics and Technology of RAS). The work at Argonne (A.G. and V.M.V) was supported by the U.S. Department of Energy, Office of Science, Basic Energy Sciences, Materials Sciences and Engineering Division. The experiments on the 20-qubit machine were performed on IBM’s

quantum computer tokyo at Oak Ridge National Laboratory and gratefully acknowledge access to this machine.

-
- ¹ M. A. Nielsen and I. L. Chuang, *Quantum Computation and Quantum Information* (2010), ISBN 9781107002173.
 - ² H. P. Breuer and F. Petruccione, *The theory of open quantum systems* (Oxford University Press, 2002).
 - ³ A. S. Holevo, *Quantum Systems, Channels, Information* (Walter de Gruyter, Berlin, 2012).
 - ⁴ S. N. Filippov, *J. Math. Sci.* **241**, 210 (2019).
 - ⁵ L. J. Landau and R. F. Streater, *Lin. Algebra Appl.* **193**, 107 (1993).
 - ⁶ K. M. R. Audenaert and S. Scheel, *New J. Phys* **10**, 023011 (2008).
 - ⁷ C. B. Mendl and M. M. Wolf, *Commun. Math. Phys.* **289**, 1057-1086 (2009).
 - ⁸ R. F. Werner and A. S. Holevo, *J. Math. Phys* **43**, 4353 (2002).
 - ⁹ S. N. Filippov and K. V. Kuzhamuratova, *Journal of Mathematical Physics* **60**, 042202 (2019), URL <https://doi.org/10.1063/1.5037700>.
 - ¹⁰ A. C. Santos, *Revista Brasileira de Ensino de Física* **39** (2016), URL <https://doi.org/10.1590/1806-9126-rbef-2016-0155>.
 - ¹¹ U. Alvarez-Rodriguez, M. Sanz, L. Lamata, and E. Solano, *Scientific Reports* **8** (2018), URL <https://doi.org/10.1038/s41598-018-33125-3>.
 - ¹² A. A. Zhukov, S. V. Remizov, W. V. Pogosov, and Y. E. Lozovik, *Quantum Information Processing* **17** (2018), URL <https://doi.org/10.1007/s11128-018-2002-y>.
 - ¹³ J. Roffe, D. Headley, N. Chancellor, D. Horsman, and V. Kendon, *Quantum Science and Technology* **3**, 035010 (2018), URL <https://doi.org/10.1088/2F2058-9565/2Faac64e>.
 - ¹⁴ M. R. Geller, *Physical Review Applied* **10** (2018), URL <https://doi.org/10.1103/physrevapplied.10.024052>.
 - ¹⁵ Y. I. Bogdanov, D. V. Fastovets, B. I. Bantysh, A. Y. Chernyavskii, I. A. Semenikhin, N. A. Bogdanova, K. G. Katamadze, Y. A. Kuznetsov, A. A. Kokin, and V. F. Lukichev, *Quantum Electronics* **48**, 1016 (2018), URL <https://doi.org/10.1070/2Fqel16760>.
 - ¹⁶ J. Morris, F. A. Pollock, and K. Modi, *Non-markovian memory in ibmqx4* (2019), URL <https://arxiv.org/abs/1902.07980>.
 - ¹⁷ IBM, *IBM Q Experience* (2016), URL <https://quantumexperience.ng.bluemix.net/>.
 - ¹⁸ M.-D. Choi, *Linear Algebra Appl.* **10**, 285 (1975).
 - ¹⁹ A. Jamiolkowski, *Rep. Math. Phys.* **3**, 275 (1972).
 - ²⁰ S. N. Filippov and K. Y. Magadov, *Lobachevskii J. Math.* **39**, 65 (2018).
 - ²¹ M. Paris and J. Řeháček, eds., *Quantum State Estimation* (Springer Berlin Heidelberg, 2004), URL <https://doi.org/10.1007/b98673>.
 - ²² IBM, *Qiskit* (2016), URL <https://qiskit.org/>.
 - ²³ R. Jozsa, *Journal of Modern Optics* **41**, 2315 (1994), <https://doi.org/10.1080/09500349414552171>, URL <https://doi.org/10.1080/09500349414552171>.